JFMSE, 36(1), pp. 21~31, 2024.
수산해양교육연구, 제36권 제1호, 통권127호, 2024.
www.ksfme.or.kr
https://doi.org/10.13000/JFMSE.2024.2.36.1.21

A Study on Ship Path Following System Utilizing a Small Model Boat

Wonjin CHOI · Serng Bae MOON†
Korea Maritime and Ocean University(researcher) · †Korea Maritime and Ocean University(professor)

소형 모형 보트를 이용한 선박 경로 추종 시스템에 관한 연구

최원진 · 문성배†
한국해양대학교(연구원) · †한국해양대학교(교수)

Abstract

This study introduces a ship path following system achieved through the design of a course controller based on the ship's maneuvering model. Both simulations and experiments were conducted to validate the system's effectiveness. The ship's maneuvering model was identified by applying an ARX (Auto-Regression with eXtra input) model, representing the system model based on input-output data. The course controller employed PD (Proportional-Derivative) controller, recognized for its simplicity and excellent control performance. Prior to sea experiments, the effectiveness of the ship's maneuvering model and course controller was verified through simulation. Subsequently, sea experiments were conducted using a small model boat. The path following results in real sea conditions revealed a maximum cross track distance (XTD) of approximately 3.4 m (3.7 L) for the experimental boat, indicating successful path following along the predefined route.

Key words : Path following system, ARX model, PD controller, Sea experiments, Small model boat

Ⅰ. Introduction

The ship's path following system is essential for safe navigation, providing automatic maneuvering and avoidance capabilities to prevent collisions with other vessels and obstacles. Research on ship path following systems, persistently advancing from the past to the present, aims to ensure secure navigation.

Son and Yoon(2009) designed a waypoint tracking algorithm for an Unmanned Surface Vessel (USV) in the form of a Rigid Inflatable Boat (RIB) and validated it through sea trials. Im and Tran (2012) focused on designing a ship track keeping algorithm for a free-running model ship, validating it through sea trials. In both studies, a notable deviation from the prescribed path was observed in the experimental results. This was compounded by the direct execution of sea trials using the designed algorithms without prior implementation of the maneuvering model of the experimental vessels and simulations.

Mou et al.(2020) designed a path following algorithm for a Water-Jetted USV. They

† Corresponding author : 051-410-4280, msbae@kmou.ac.kr
* This research was supported by the 'Development of Autonomous Ship Technology (20200615)' funded by the Ministry of Oceans and Fisheries (MOF, Korea).

implemented ship equations of motion considering the vessel's three degrees of freedom, evaluated the designed algorithm through simulations, and then conducted experiments based on it. The experimental vessel effectively followed the prescribed path, but there were limitations to the experiments as they were conducted in a still water tank, lacking environmental disturbances such as wind, waves, currents, or other external factors. Additionally, there were challenges in implementing the ship equations of motion for simulations, requiring coefficients related to maneuvering motion.

In this study, the authors designed a ship path following system and validated the system through simulations and experiments using a small-scale model boat. The results of simulations and experiments serve as the verification of the proposed system.

The ship's maneuvering motion model for simulation can be simplified by employing system identification methods, which mathematically model the system using the ship's input-output data. For the path following, a Proportional-Derivative (PD) controller was employed to control the course of the experimental boat.

Simulation was utilized to validate the effectiveness of the maneuvering model for the experimental boat. Based on this validation, the parameters of the course controller were tuned to enable accurate path tracking by the experimental boat without inducing significant deviations.

In conclusion, sea experiments with the experimental boat were conducted in a real-world marine environment. The analysis of the path following results validated the effectiveness of the path following system.

Ⅱ. Methods

1. Experimental boat

For research purposes, the commercially available RC model boat, the Sonicwake 36" Self-Righting Brushless Deep-V RTR manufactured by Pro Boat, was modified and utilized in the study.

The experimental boat, illustrated in [Fig. 1], features a monohull design with a length of less than 1 m and a weight of approximately 4.5 kg. It is characterized by the rudder being offset to starboard rather than directly behind the propeller.

Additionally, with the housing attached to the upper part of the hull for additional equipment, it exhibits a relatively large windage area. As a result, it is susceptible to the effects of wind and waves in maritime conditions.

(a) (b)

[Fig. 1] The overall. (a) and stern (b) appearance of the experimental boat.

Built-in equipment includes a Brushless Direct Current (BLDC) motor, an Electronic Speed Controller (ESC), and a propeller for propulsion, as well as a servo motor and rudder for steering. Furthermore, there is a Radio Frequency (RF) receiver for wireless remote control of the boat.

Additionally, a Global Positioning System (GPS) module and an Attitude and Heading Reference System (AHRS) module were equipped to collect

data such as the position, heading, speed, and yaw angle of the experimental boat. A microcomputer was also incorporated to calculate the target course based on the collected data and control the boat accordingly. The detailed specifications of the experimental boat are presented in <Table 1>.

The AHRS module was utilized to acquire the heading information of the experimental boat, with a heading error of 1.5° under dynamic conditions, as specified by the manufacturer.

The GPS module was employed to obtain data, including the position, speed, and course of the experimental boat. Under dynamic conditions, the manufacturer specifies errors of 2.5 m for position, 0.05m/s for speed and 0.3° for course.

The SBC used in this study is the LattePanda, equipped with Windows 10. This SBC features an Intel Atom processor and 4GB of Random Access Memory (RAM), with the added advantage of integration with the Arduino Leonardo microcontroller, enabling versatile connections with various sensors.

<Table 1> Particulars of experimental boat

Items	Features
Hull type	Monohull
Dimensions	914 mm × 279 mm × 240 mm
Draft	7 cm
Weight	4.5 kg
Speed	50+ kn
Built-in equipment	BLDC motor, ESC, Propeller, Servo motor, Rudder, RF receiver
Additional equipment	GPS module, AHRS module, SBC

2. Path following system

For path following, a course controller is essential, and understanding the ship's maneuvering model is key to its design. This section explains the process of identifying the experimental boat's maneuvering model and designing the course controller.

A. Ship maneuvering model

The maneuvering of a ship is represented by the yaw angular velocity, which is the output, corresponding to the rudder angle, the input. By measuring both values, the mathematical model of the system can be obtained. Commonly used model structures for linear systems include Auto Regressive (AR) models, AutoRegression with eXtra input (ARX) models, Output Error (OE) models, Box-Jenkins (BJ) models, etc.

In this study, the ARX model was employed to obtain the system model through input and output data, allowing for relatively easy determination of values of system parameters compared to other models. The ARX model expresses the output at the current time as the sum of a function of the previous time's output, current and previous time's inputs, and the white noise.

In the time domain, when a single input data $u(t)$ at time t results in a single output data $y(t)$, an ARX model, including possible errors $e(t)$ other than the input and output, can be represented using the delay operator q as shown in Eq. (1) (Ljung, 1987).

$$A(q)y(t) = B(q)u(t-nk) + e(t) \quad \cdots\cdots\cdots\cdots\cdots (1)$$

Here, $A(q) = 1 + a_1 q^{-1} + a_2 q^{-2} + \cdots + a_{na} q^{-na}$

$$B(q) = b_1 + b_2 q^{-1} + b_3 q^{-2} + \cdots + b_{nb} q^{-nb+1}$$

Where, $y(t)$ is the output at time t, $u(t)$ is the input at time t, $e(t)$ is the white-noise disturbance value, na is the number of poles, nb is the number of zeros, nk is the dead time in the system.

To achieve the optimal ARX model, it is essential to carefully choose the model's order. Excessive order may cause overfitting, yielding a poorly generalized model. Conversely, overly simplified models may lead to underfitting, hindering accurate representation.

To determine the optimal order, various criteria like Akaike's Information Criterion (AIC), Bayesian Information Criterion (BIC), Minimum Description Length (MDL), etc., can be used. These methods calculate scores for different models, facilitating the selection of the optimal one and preventing overfitting by imposing penalties on complexity.

AIC tends to favor complex models and may be less accurate with larger sample sizes, while BIC generally selects simpler models, but its outcomes can be influenced by sample size. In contrast, MDL aims to prevent overfitting by choosing simple and explanatory models, enhancing generalization to the data, albeit with the trade-off of complex computations.

The study aims to derive a concise and comprehensive maneuvering model for ships, utilizing Rissanen's MDL criterion, Eq. (2), to select the model that succinctly explains the data (Rissanen, 1978; The MathWorks Inc., 2023).

$$V_{\mathrm{mod}} = V\left(1+\frac{d\log(N)}{N}\right) \quad \cdots\cdots (2)$$

Where, V is the loss function, d is the total number of parameters in the structure, N is the number of data points used for the estimation. The orders of parameters na and nb in the ARX model are varied to calculated the MDL values. The model with the smallest calculated MDL value is selected as the optimal model. The parameters a_{na} and b_{nb} are estimated using the least squares method.

As for the predictive performance evaluation of the ARX model, commonly used methods include Root Mean Square Error (RMSE) and Normalized Root Mean Square Error (NRMSE). RMSE reflects the absolute error magnitude, influenced by measurement units. Conversely, NRMSE normalizes observed values, providing a measure of relative prediction accuracy independent of units. Utilizing both metrics allows a comprehensive evaluation of the model's performance from different perspectives. RMSE and NRMSE are expressed as Eq. (3) and Eq. (4), respectively.

$$\mathrm{RMSE} = \sqrt{\frac{1}{n}\sum_{i=1}^{n}(y_i-\hat{y_i})^2} \quad \cdots\cdots (3)$$

$$\mathrm{NRMSE} = \frac{\mathrm{RMSE}}{\mathrm{Max}(y_i)-\mathrm{Min}(y_i)} \quad \cdots\cdots (4)$$

Where, y_i represents the actual measured values, $\hat{y_i}$ corresponds to the values estimated through the model, $\mathrm{Max}(y_i)$ is the maximum value of y_i, $\mathrm{Min}(y_i)$ is the minimum value of y_i, and n signifies the number of measured samples. RMSE and NRMSE approaching 0 indicate that the values calculated through the model are similar to the actual values.

B. Course controller

The ship's course controller should adapt to factors such as the shallow water effect and various environmental conditions that may influence the ship's maneuvering performance, such as turning

ability and course keeping ability. It should ensure precise, quick course changes, avoiding overshoot, particularly during significant yaw angle changes (Fossen, 1999).

In this study, Proportional-Derivative (PD) controller was used to eliminate integral action, preventing system divergence and error accumulation. PD control, known for reducing overshoot, facilitates simpler coefficient settings.

Additionally, due to the small size of the experimental boat, significant drift angles result from external forces like wind and currents, causing a notable difference between the heading angle and the Course Over Ground (COG). To ensure accurate path following, COG was used as the control variable for the controller instead of the heading angle. [Fig. 2] illustrates the block diagram of the PD controller utilized in this study.

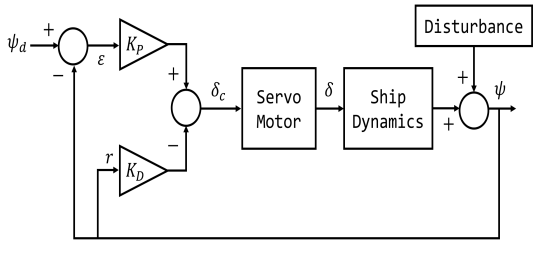

[Fig. 2] Block diagram of PD controller.

Where, K_P is the proportional gain, K_D is the derivative gain, ψ_d is the target course, ψ is the current course, e is the course error, r is the yaw angular velocity, δ_c is the target rudder angle and δ is the current rudder angle.

The synthesis of hull motion due to steering and external forces results in current course(ψ), obtained from GPS. The current course(ψ) is fed back to the controller, which calculates the target rudder(δ_c) angle to reduce the course error(e). The target rudder angle(δ_c) is input to the servo motor, which moves the rudder to the angle commanded by the controller. Eq. (5) represents the PD controller formula for calculating the target rudder angle.

$$\delta_c = K_P(\psi_d - \psi) - K_D \times r \quad \cdots\cdots\cdots\cdots\cdots\cdots\cdots\cdots\cdots\cdots \quad (5)$$

The parameters of a PD controller must be appropriately tuned based on the system's characteristics and operating environment. This tuning process establishes suitable parameter values, enabling the design of a responsive controller tailored to the controlled system's characteristics.

One of the representative methods for tuning the parameters of a PD controller is the two methods proposed by Ziegler and Nichols (1942). Setting parameters through these tuning methods usually yields satisfactory controller performance, though optimal performance is not guaranteed. It is crucial to validate the controller's performance post-design using these methods, and if needed, fine-tuning of parameters may be necessary (Chung, 2018).

The first method in this tuning technique uses a step input to measure the output response of the target plant, extracting characteristic coefficients for setting the PD controller parameters. Since its applicability is limited to stable systems or those not including an integral component, it is not suitable for this study. Therefore, the second method, the ultimate sensitivity method, was chosen for controller tuning.

In the ultimate sensitivity method, a closed-loop circuit is created by introducing proportional action to the system. Applying a step input and progressively increasing the proportional gain from zero results in sustained oscillations in the output.

The proportional gain value at which sustained oscillations occur is termed the ultimate gain ($K_u = K_P$), and the output's oscillation period is the ultimate period (T_u). These values are then used to determine the controller parameters, as shown in Eq. (6) and Eq. (7) (Ziegler and Nichols, 1942; McCormack and Godfrey, 1998).

$$K_P = 0.8K_u \quad \cdots\cdots (6)$$

$$K_D = 0.10K_u T_u \quad \cdots\cdots (7)$$

The obtained parameters are used as the initial values for controller tuning, and fine-tuning is performed to set the parameters that represent the optimal response for the system.

Ⅲ. Results

1. maneuvering model identification

Sea experiments were conducted to gather data on the input rudder angle and output yaw angular velocity. A range of rudder angles, up to 35 degrees, was employed to collect corresponding data on the yaw angular velocity. The experiments conducted in the vicinity of the connection area with the Korea Maritime and Ocean University (KMOU). During the experiment, wave height was less than 0.3 m, and wind speed was observed at 2.0 m/s.

A total of around 10 minutes and 25 seconds of data were collected, with 70% (438 seconds) used for model identification and the remaining 30% (187 seconds) for model validation.

First, to determine the order of the ARX model, the orders of na and nb were varied from 1 to 10, and the MDL values were calculated. The results are presented in [Fig. 3].

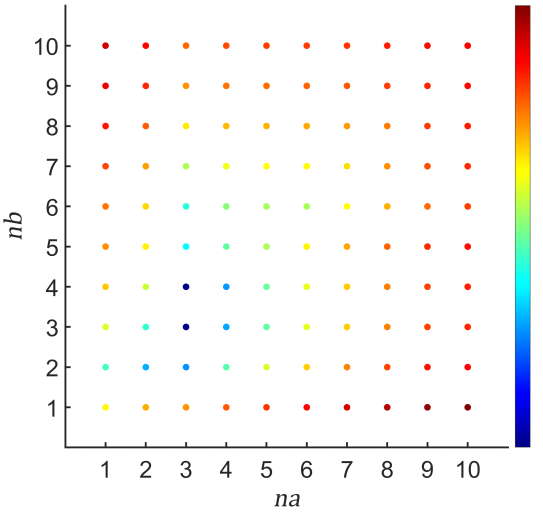

[Fig. 3] Variation of MDL values with respect to the order of the ARX model.

The MDL value was minimized to 13.3751 at $na = 3$, $nb = 4$. The ARX model with three poles and four zeros, expressed as the transfer function from the input rudder angle to the output yaw angular velocity, is represented by Eq. (8).

$$\frac{r}{\delta}(z) = \frac{0.4708q^{-1} - 0.1219q^{-2} - 0.0822q^{-3} - 0.07686q^{-4}}{1 - 0.206q^{-1} - 0.1421q^{-2} - 0.2487q^{-3}} \quad \cdots\cdots (8)$$

The acquired ARX model was validated by comparing the actual yaw angular velocity from the remaining 30% of the data with the predicted values from the model. The RMSE was 6.4424, and the NRMSE was 0.2085. Given the experimental boat's small size and light weight, making it susceptible to external forces, the ARX model is considered effective in predicting the actual yaw angular velocity.

2. Controller parameter tuning

The maneuvering model of the experimental boat was used for PD controller tuning to optimize control parameters. The ultimate sensitivity method was applied, using a step input of magnitude 10 and incrementally increasing the proportional gain (K_P). Continuous oscillations were observed in the experimental boat when the proportional gain reached 1.7, as illustrated in [Fig 4], with a corresponding period of 7 seconds.

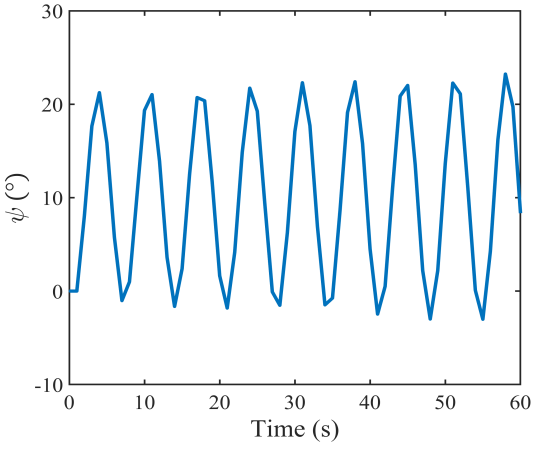

[Fig. 4] PD controller parameter tuning.

The initial controller parameters were computed using the critical gain ($K_u = 1.7$) and critical period ($T_u = 7$) values obtained from the ultimate sensitivity method. Subsequent fine-tuning was carried out based on these initial parameters, setting the proportional gain (K_P) to 0.8 and the derivative gain (K_D) to 1.6.

3. Simulations

A. maneuvering model verification results

To validate the ship maneuvering model, turning simulations were performed with rudder angles set to 25 degrees starboard and 30 degrees port. The results were compared and analyzed alongside the actual turning experiment results from section 1 of this chapter, as shown in [Fig. 5].

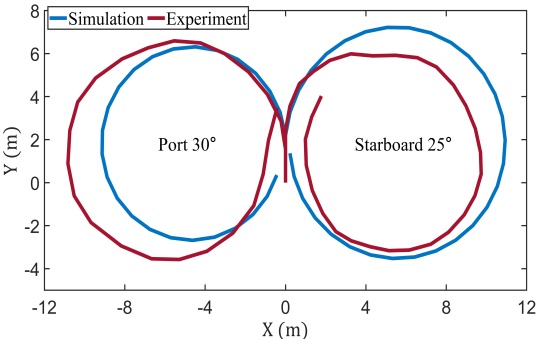

[Fig. 5] Comparison between simulation and actual turning trajectories.

The blue solid line represents the simulated turning trajectory based on the identified maneuvering model, while the red line depicts the actual turning trajectory from the experimental boat turning. When turning starboard with a 25-degree rudder angle, the simulation's turning radius was about 1.2 m (1.3 L) larger than the experimental turning radius. In contrast, when turning port with a 30-degree rudder angle, the simulation's turning radius was approximately 1.7 m (1.9 L) smaller than the experimental turning radius.

The turning circle disparity between the experiment and simulation is rooted in the linear regression model employed for ship maneuvering in the simulation. This model suggests equal turning circles on both port and starboard sides when turning at the same rudder angle. However, real single-screw vessels exhibit slight variations in the turning circle due to factors like suction current, discharging current, and sidewise pressure, depending on whether the turn is to port or

starboard (Yoon, 2019).

Typically, in single-screw vessels, the turning circle is larger on the side of the propeller rotation(Jung, 2008; Kim, 2005). Notably, our experimental boat, with the rudder positioned to the right of the propeller, exhibits a smaller than usual starboard turning circle, deviating from this general pattern.

Although there is a slight difference in turning radii between the simulation and the experiment, about 1 m (1.1 L), it is considered negligible when analyzing the overall yaw motion of the experimental boat.

B. Path following verification results

Using the identified maneuvering model and designed controller, a path following simulation was performed for the experimental boat. Considering the size of the area where the sea trial took place, the simulation was set to navigate in a clockwise direction, starting from the departure point and following seven waypoints, as shown in <Table 2>.

<Table 2> List of waypoints for simulation

	X(m)	Y(m)	Course(°)	Distance(m)
Start	10.0	15.0		
			000	35.0
WP1	10.0	50.0		
			018	40.0
WP2	22.4	88.0		
			076	50.0
WP3	70.9	100.1		
			126	37.9
WP4	101.6	77.8		
			182	39.0
WP5	100.2	38.8		
			228	37.0
WP6	72.7	14.0		
			271	49.0
WP7	23.7	14.9		

[Fig. 6] depicts the simulation trajectory of the experimental boat. Star-shaped symbols represent waypoints, dashed lines connect waypoints in a straight line, and the blue solid line represents the trajectory of the experimental boat.

In the path following simulation, the experimental boat deviated approximately 1 m (1.1 L) at waypoint 2 and 1.2 m (1.3 L) at waypoint 4. However, overall, the boat navigated well along the designated path.

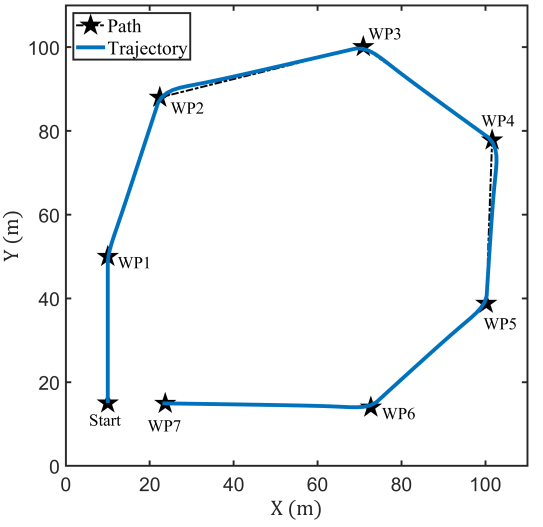

[Fig. 6] Path following simulation trajectory of the experimental boat.

4. Sea experiments

The sea experiments for path following of the experimental boat was conducted in the vicinity of the connection area with the KMOU. <Table 3> shows the list of waypoints for sea experiments, which were set considering the experimental area.

The alter course angle was less than 60° starboard, and waypoint distances ranged from 35 to 51 m. [Fig. 7] displays a satellite image of the

experimental area with marked waypoints. The area is open to the north, with wave height below 0.2 m, and wind speed at 1.8 m/s during the experiment. Boat rpm remained constant throughout the experiment.

<Table 3> List of waypoints for sea experiments

	Latitude (°)	Longitude (°)	Course (°)	Distance (m)
Start	35.074771	129.085466		
			245	35.5
WP1	35.074639	129.085111		
			260	38.8
WP2	35.074580	129.084690		
			318	50.6
WP3	35.074920	129.084320		
			008	37.6
WP4	35.075255	129.084377		
			064	39.0
WP5	35.075407	129.084763		
			110	37.3
WP6	35.075290	129.085148		
			153	48.6
WP7	35.074896	129.085379		

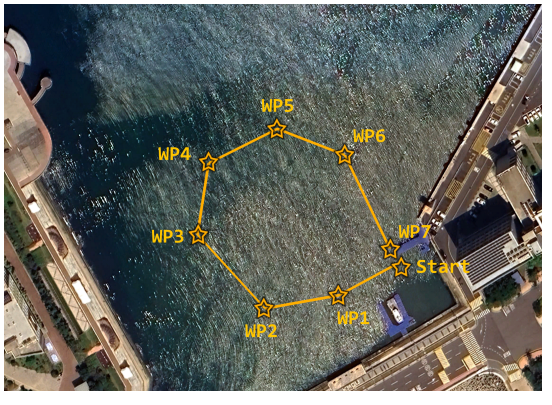

[Fig. 7] Experimental area with waypoints.

[Fig. 8] depicts the trajectory of the experimental boat during the sea experiment. The acquired latitude and longitude coordinates through the GPS module were transformed from the WGS84 coordinate system to the Universal Transversal Mercator (UTM) coordinate system, a single-plane coordinate system encompassing the entire Korean Peninsula, using the QGIS program.

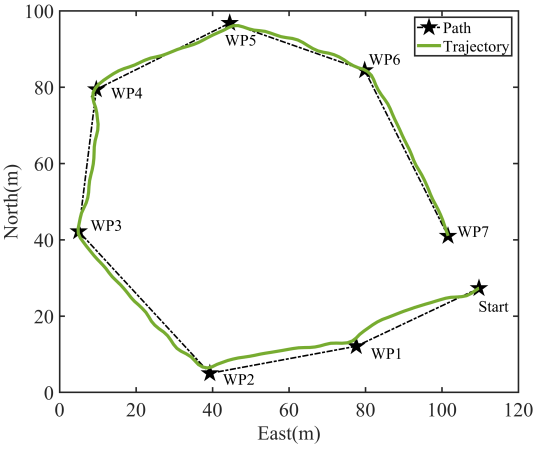

[Fig. 8] Sea experimental trajectory for path following of the experimental boat.

The star symbols denote waypoints, connected by dashed lines, and the solid green line shows the experimental boat's trajectory. Although some deviation was observed during navigation from the starting point to waypoint 2, overall, the boat adhered closely to the designated path.

[Fig. 9] displays the cross track distance (XTD), yaw angle, and speed of the experimental boat over time. Vertical dashed lines in each graph mark the moments the boat passes waypoints 1, 2, 3, 4, 5, and 6.

The maximum XTD for the experimental boat was 3.4 m (3.7 L), occurring between the starting point and waypoint 1. Subsequently, the XTD remained below 3m (3.3 L) for the remaining path. Given the GPS module errors (2.5 m) and the small size of the boat susceptible to maritime conditions, the observed XTD during the experiment is

considered insignificant.

The experimental boat maintained a course within approximately 10 degrees between waypoints, using a maximum rudder angle of 35 degrees to change course when passing through waypoints. Despite maintaining a constant motor rpm, speed oscillations occurred, likely influenced by wind and waves.

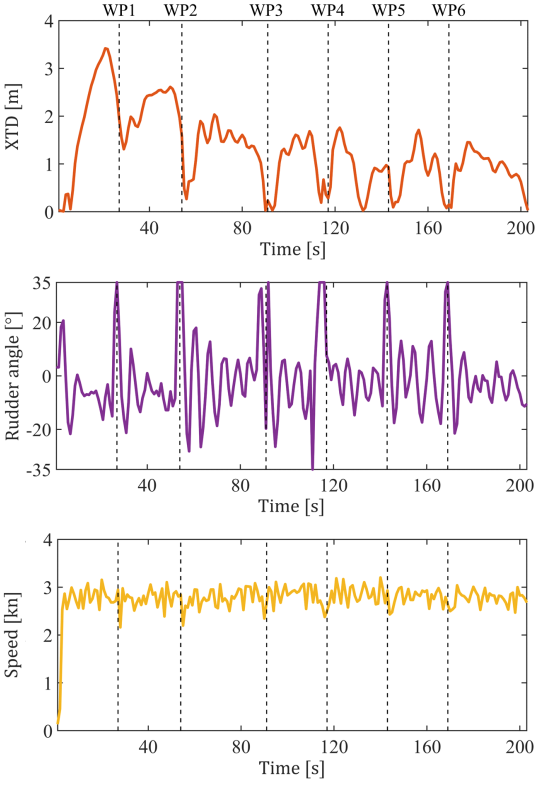

[Fig. 9] Experiment result.

Ⅳ. Conclusion

In this study, the authors implemented a ship's path following system. Simulations and sea trials were conducted using a commercially available small-scale model boat to validate its effectiveness. The key points of our research include:

1. The ship's maneuvering model was identified using yaw angles and yaw angular velocities data only. Turning simulations validated that the identified model appropriately represents the experimental boat's maneuvering behavior.

2. A PD control based course controller was designed, and path following simulations were performed. Path following simulations validated that the designed course controller enables the experimental boat to effectively follow a predefined path.

3. Sea trials were conducted using a small-scale model boat. The experimental boat successfully followed a predefined seven waypoints with minor deviation.

In this study, using a small-scale model boat presented challenges due to significant maritime influences, introducing noise during sea data acquisition. However, through simulation-guided efficient tuning of PD controller coefficients based on a ship maneuvering model, the experimental boat demonstrated effective path following during sea trials, closely adhering to the predetermined route, despite maritime challenges.

In future studies, we plan to apply the developed approach to boats or vessels of practical operational size. The identification of the ship's maneuvering model, which does not depend on challenging-to-obtain data such as fluid dynamic coefficients, implies its potential suitability for general vessels. We anticipate that these advancements will contribute to the development of path-following systems.

References

Chung DW(2018). Automatic control engineering : using CEMTOOL, MATLAB. Dooyangsa, Seoul,

Korea.

Fossen TI(1999). Recent developments in ship control systems design. World Superyacht Review.

Go SH(2012). Introduction and basic theory of system identification. Institute of Control, Robotics and Systems, 18(2), 33~38.

Im NK and Tran VL(2012). Experiment on Track-keeping Performance using Free Running Model Ship. Journal of the Korean Society of Marine Environment & Safety, 18(3), 221~226. https://doi.org/10.7837/kosomes.2012.18.3.221

Jung CH, Lee HK and Kong GY(2008). A Study on the Ship's Performance of T.S. HANBADA(Ⅲ) - The Evaluation of Maneuvering Performance with Actual Ship Trials -. Journal of Navigation and Port Research, 32(6), 439~445. https://doi.org/10.5394/KINPR.2008.32.6.439

Kim MS, Shin OH, Kang KM and Kim MS(2005). Varation of the Turning Circle by Rudder Anlge and the Ship's Speed – Mainly on the Training Ship KAYA -. Journal of Korean Society of Fisheries Technology, 41(2), 156~164. https://doi.org/10.3796/KSFT.2005.41.2.156

Ljung L(1987). System identification: Theory for the user. PTR Prentice Hall.

McCormack AS and Godfrey KR(1998). Rule-based autotuning based on frequency domain identification. IEEE transactions on control systems technology, 6(1), 43~61. https://doi.org/10.1109/87.654876

Mou J, He Y, Zhang B, Li S and Xiong Y(2020). Path following of a water-jetted USV based on maneuverability tests. Journal of Marine Science and Engineering, 8(5), 354. https://doi.org/10.3390/jmse8050354

Rissanen J(1978). Modeling by shortest data description. Automatica, 14(5), 465~471. https://doi.org/10.1016/0005-1098(78)90005-5

Son NS and Yoon HK(2009). Study on a Waypoint Tracking Algorithm for Unmanned Surface Vehicle (USV). Journal of navigation and port research, 33(1), 35~41. https://doi.org/10.5394/KINPR.2009.33.1.035

The MathWorks Inc.(2023). Select model order for single-output ARX models. Natick, Massachusetts: The MathWorks Inc. https://kr.mathworks.com/help/ident/ref/selstruc.html

Yoon JD(2019). Ship Control: Theory and Practice. EDUSEJONG, Busan, Korea.

Ziegler JG and Nichols NB(1942). Optimum Settings for Automatic Controllers. Transactions of the American society of mechanical engineers, 64(8), 759~765. https://doi.org/10.1115/1.4019264

• Received : 27 November, 2023
• Revised : 15 December, 2023
• Accepted : 21 December, 2023